Predicted properties of Delbrück scattering for photon energies up to 10^4 MeV

P. Rullhusen, J. Trube,* A. Baumann, K. W. Rose, F. Smend, and M. Schumacher
II. Physikalisches Institut der Universität Göttingen, D-3400 Göttingen, Federal Republic of Germany
(Received 2 March 1987)

Using an exact numerical evaluation of the lowest-order Feynman graphs and the impact-factor approximation of Cheng and Wu for the lowest-order as well as the multiphoton-exchange Feynman graphs, properties of Delbrück scattering are investigated at energies between 1 and 10^4 MeV. The predicted scaling behavior starts showing up above about 100 MeV, i.e., at much higher energies than previously anticipated. At angles below 30° the amplitudes are predominantly imaginary and are modified by multiphoton exchange by factors of 2 to 4. At angles above 90° real and imaginary parts are of the same magnitude at all energies. Discrepancies observed between the predictions of the exact numerical evaluation of the lowest-order Feynman graphs and the impact-factor approximation to the lowest-order amplitudes make a reinvestigation of computational methods for the Coulomb-correction effect highly desirable.

I. INTRODUCTION

Delbrück (D) scattering, i.e., the elastic scattering of photons in the Coulomb field of a nucleus, has been discussed for several different reasons. (i) For nuclear-structure studies carried out using the method of photon scattering, D scattering is a background process which has to be taken care of in order to arrive at the genuine nuclear-structure information.[1,2] D scattering and elastic nuclear scattering are coherent processes, with the D-scattering component being dominant for heavy nuclei and forward angles. Below 10 MeV D scattering is observed up to scattering angles of 180°, whereas above 100 MeV the intensity is forward-peaked within a few degrees. (ii) From the point of view of quantum electrodynamics (QED), D scattering offers a clear-cut access to vacuum polarization in the presence of strong electric fields.[3,4] By a precise measurement[3,5] of elastic differential cross sections at the photon energy 2.75 MeV it was possible to test a single Feynman graph of the order Z^2e^6 with an accuracy of 5%. This is the highest accuracy ever achieved for a Feynman graph of this high order. (iii) Furthermore, D scattering as well as photon splitting may serve as gauge-invariant tests of the QED electron propagator, since the D Feynman graphs contain closed electron loops.[6–8]

The first reliable calculations of D amplitudes were carried out in the early 1970s. Papatzacos and Mork[9,10] calculated D amplitudes in the lowest-order Born approximation from the fourth-rank vacuum-polarization tensor using conventional Feynman techniques and gauge invariance. De Tollis and co-workers[11–14] have calculated the fourth-rank vacuum-polarization tensor numerically in terms of rational, logarithm, and dilogarithm functions using double dispersion relations. Because of these efforts, numerical data have been obtained[3,9–15] for the lowest-order D amplitudes for energies up to 70 MeV.

Using the impact-factor method, Cheng and Wu[16,17] arrived at imaginary parts of lowest-order D amplitudes, valid asymptotically at photon energies much larger than the electron mass and for fixed nonzero momentum transfer. By replacing the photon propagator entering into the formula for the lowest-order amplitude by a modified expression, the exchange of an arbitrarily large number of photons with the nucleus, i.e., the Coulomb-correction effect, was taken into account.

An interesting property of the D amplitudes was discussed by Cheng, Tsai, and Zhu.[18] Calculating the lowest-order D amplitude without approximations, they found that for fixed angle θ the amplitude scales in the form $\omega^{-1}f(\theta)$ as $\omega/m\rightarrow\infty$, where ω is the photon energy and m the electron mass. In addition, they proved that this scaling behavior is expected to occur also when the Coulomb-correction effect is included. As a test they analyzed[18] experimental data in the energy range around 10 MeV and found a strong conflict with the scaling laws. This conflict has later been partly removed by the present authors[19] by properly disentangling the experimental data in terms of D amplitudes and nuclear amplitudes.

The present work has been carried out for several reasons. (i) One aim is to arrive at predictions of D amplitudes at intermediate energies, i.e., between the low-energy domain below 30 MeV and the high-energy domain above 1 GeV. Both the low-energy[20,21] and the high-energy[4] domains were subject to previous investigations, whereas the intermediate-energy range is largely unexplored. From a nuclear-physics point of view this energy range is of special interest for elastic photon-scattering studies, since information is expected about pions in complex nuclei[2] and about the modification of the nucleon polarizability due to the nuclear medium,[22] which are not available from any other type of investigation. (ii) Apart from this practical aspect, it is our intention to arrive at quantitative information about the validity of the scaling law found by Cheng, Tsai, and Zhu.[18] Up to now it has been known only vaguely at what photon energies ω the scaling behavior is expected to show up.

For the purpose of these investigations the formulas provided by De Tollis and Pistoni[13] and by Cheng and Wu[17] have been evaluated by Monte Carlo procedures.

II. NUMERICAL EVALUATION OF THE LOWEST-ORDER FEYNMAN GRAPH

We use the following conventions for the D amplitudes:

$$\frac{d\sigma}{d\Omega}=\tfrac{1}{2}(\,|A_\parallel|^2+|A_\perp|^2)(Z\alpha)^4 r_0^2 \tag{1a}$$

$$=(\,|A_{++}|^2+|A_{+-}|^2)(Z\alpha)^4 r_0^2\,, \tag{1b}$$

with $\alpha=e^2/4\pi$ the fine-structure constant ($\hbar=c=1$), $r_0=e^2/4\pi m$ the classical electron radius, and Z the atomic-charge number. The scattering amplitudes $A_{\parallel,\perp}$ for linear polarization are related to the helicity amplitudes $A_{++,+-}$ via

$$A_\parallel=A_{++}+A_{+-}\,, \tag{2a}$$

$$A_\perp=A_{++}-A_{+-}\,. \tag{2a}$$

In order to extend existing tabulations[3,9–15] of lowest-order D amplitudes to higher energies we evaluated numerically the following expressions derived by De Tollis and Pistoni:[13]

$$\operatorname{Im} A_{\substack{++\\+-}}(d,p)=\frac{1}{\pi p}\int_1^{k^2/4}dy\int_{x_-}^{x_+}dx\int_0^b dz\; A_\pm(x,y,z;d,p) \tag{3}$$

with $k=\omega/m$, θ the scattering angle, $d=k\sin(\theta/2)$, $p=k\cos(\theta/2)$, $x_\pm=[p\pm(k^2-4y)^{1/2}]^2$, and $b=(1-1/y)^{1/2}$.

The integrands $A_\pm(x,y,z;d,p)$ are irrational functions of their arguments and are given explicitly by De Tollis and Pistoni.[13] The integration has been carried out using a Monte Carlo technique. Appropriate substitutions of the integration variables as described in Ref. 14 have been used in order to reduce the region of integration to a unit cube and to reduce the variance of the calculated integrals in each iteration step of the Monte Carlo procedure. Typically, the integration volume was subdivided into 64 subvolumes of equal size, and in each of them the integrand was evaluated at 200 points. Except for very high energies ω, convergence of better than 1% was obtained in less than 50 iteration steps, corresponding to 1 minute of CPU time on a Cray-1. All calculations have been performed in 64-bit arithmetic. For high energies ω the variance of the integrals is given by error bars in Figs. 1–7.

The calculations of the real parts of the lowest-order amplitudes involve the evaluation of a fourfold integral as described in Refs. 13 and 14. Since these calculations are very time consuming and since for the cases of our interest the real parts are much smaller than the imaginary parts, we made no effort to supplement the existing tabulations.

III. NUMERICAL EVALUATION OF THE HIGH-ENERGY APPROXIMATION

In the limit of high energies ω and for fixed nonvanishing momentum transfer $\Delta=2\omega\sin\theta/2$ the D amplitudes can be calculated to all orders in $(Z\alpha)$ using the impact-factor method derived by Cheng and Wu.[16,17] Applying the convention given by (1a) the expression derived by Cheng and Wu[17] for the D amplitudes can be rewritten as

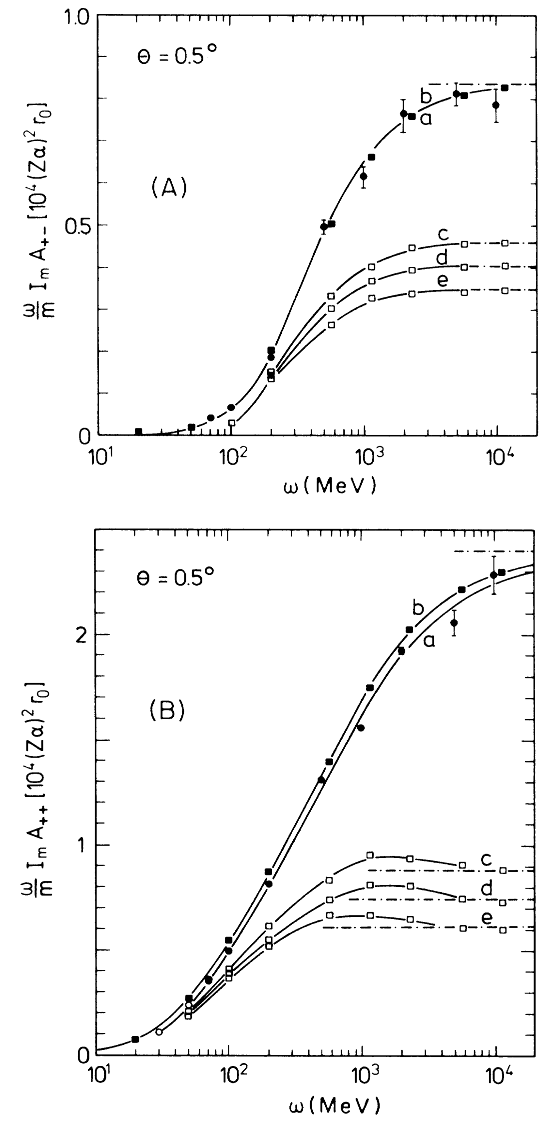

FIG. 1. Amplitudes for Delbrück scattering through $\theta=0.5°$ multiplied by ω/m. (A) Scattering with helicity flip, (B) scattering without helicity flip. a imaginary lowest-order amplitude calculated from the exact evaluation of the lowest-order Feynman graph (3). b imaginary lowest-order amplitude calculated using the impact-factor method (4) and (6). c–e imaginary Coulomb-corrected amplitudes calculated for $Z=73$, 82, 92, respectively, using the impact-factor method (4). f real lowest-order amplitude calculated from the exact evaluation of the lowest-order Feynman graph (not shown in Figs. 1 and 4). Dash-dotted curves indicate high-energy limits (8).

$$A_{\parallel,\perp}=-\frac{i}{\pi}\frac{\omega}{m}\frac{\sinh(\pi Z\alpha)}{\pi Z\alpha}\int_0^1 dx\int_0^1 d\sigma\int_0^1 dz\int_0^{1/2} dz'\cos\left[Z\alpha\ln\frac{1-z'}{z'}\right][f(x,\sigma,z,z';\Delta)+g_{\parallel,\perp}(x,z)h(x,\sigma,z,z';\Delta)] \quad (4)$$

with f,h being rational functions of their arguments as given in Ref. 17, and

$$g_{\parallel}=1-8z(1-z)x(1-x)\ , \quad (5a)$$

$$g_{\perp}=1\ . \quad (5b)$$

Equation (4) is valid in the limits $\omega \gg m$ and $\Delta \gg m^2/\omega$. Contributions to D scattering involving multiphoton exchange (Coulomb-correction terms) are included in (4) to all orders in $(Z\alpha)$. The lowest-order D amplitudes can be obtained in the limit of small charge numbers using

$$\lim_{Z\alpha\to 0}\frac{\sinh(\pi Z\alpha)}{\pi Z\alpha}\cos\left[Z\alpha\ln\frac{1-z'}{z'}\right]=1\ . \quad (6)$$

As can be seen from (4), the real parts of the D amplitudes vanish in this asymptotic limit. The quantities $(1/\omega)A_{\parallel,\perp}$ are functions of the mometum transfer Δ only and, therefore, the same is true for

$$\frac{d\sigma}{dt}=\frac{\pi}{\omega^2}\frac{d\sigma}{d\Omega}\ . \quad (7)$$

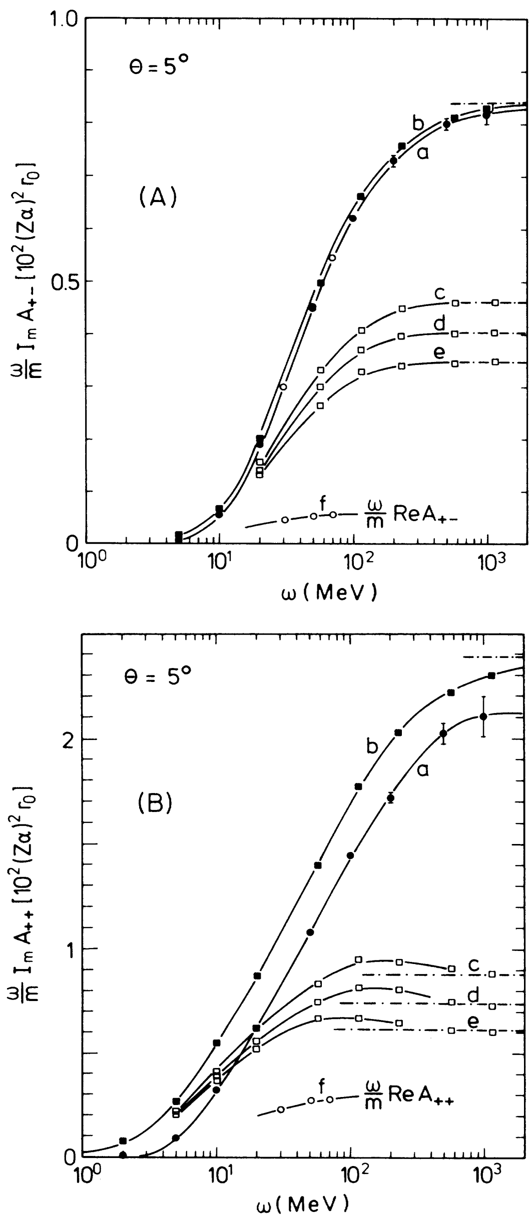

FIG. 2. Same as in Fig. 1 but for $\theta=5°$.

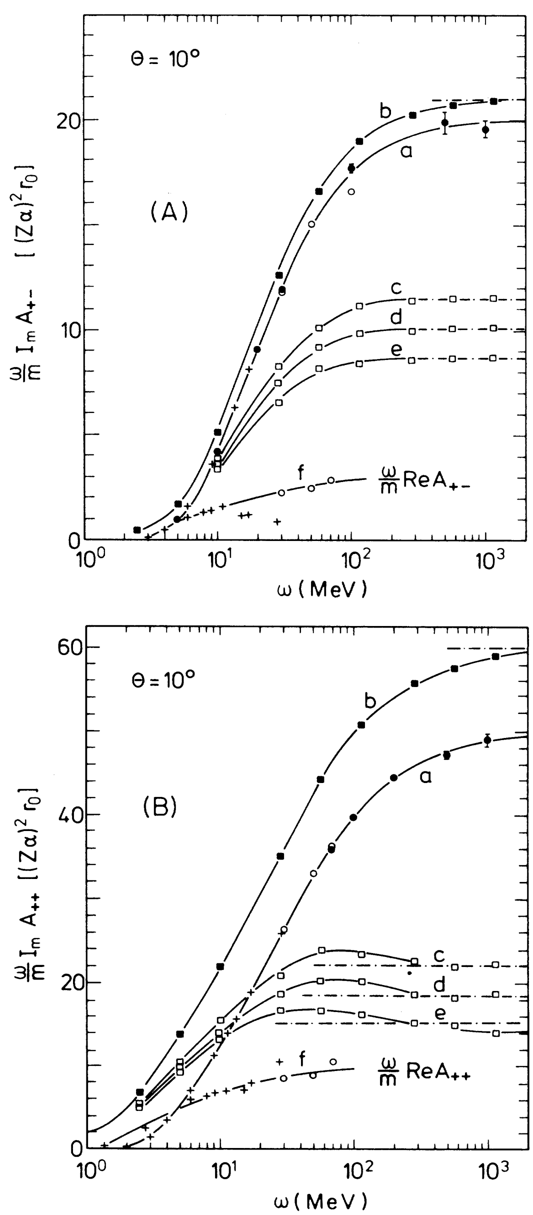

FIG. 3. Same as in Fig. 1 but for $\theta=10°$.

In the case of high energies ω and small scattering angles θ, i.e., $\omega \gg \Delta \gg m$ or $1 \gg 2\sin\theta/2 \gg m/\omega$, (4) can be integrated analytically giving[17]

$$A_{\parallel,\perp} \sim -\frac{i}{\pi}\frac{\omega m}{\Delta^2}\left[-\frac{2}{3}\frac{1\mp 3(Z\alpha)^2}{(Z\alpha)^2} + \frac{8\pi^2}{3}[1-2(Z\alpha)^2]\frac{\operatorname{csch}(2\pi Z\alpha)}{2\pi Z\alpha} \mp 2(Z\alpha)\operatorname{Im}\Psi'(1-iZ\alpha)\right]. \quad (8)$$

Equation (8) may be replaced[17] by a simpler expression in the limit $Z\alpha \to 0$. When comparing (4) and (8) with the corresponding expressions of Ref. 17, consideration has to be given to the fact that the amplitudes $A_{\parallel,\perp}$ of this paper are smaller by a factor $1/4\pi$ than the corresponding amplitudes given by Cheng and Wu.[17]

We evaluated the fourfold integral of (4) by a Monte Carlo technique. This calculation was straightforward except for the non-helicity-flip amplitudes A_{++} including

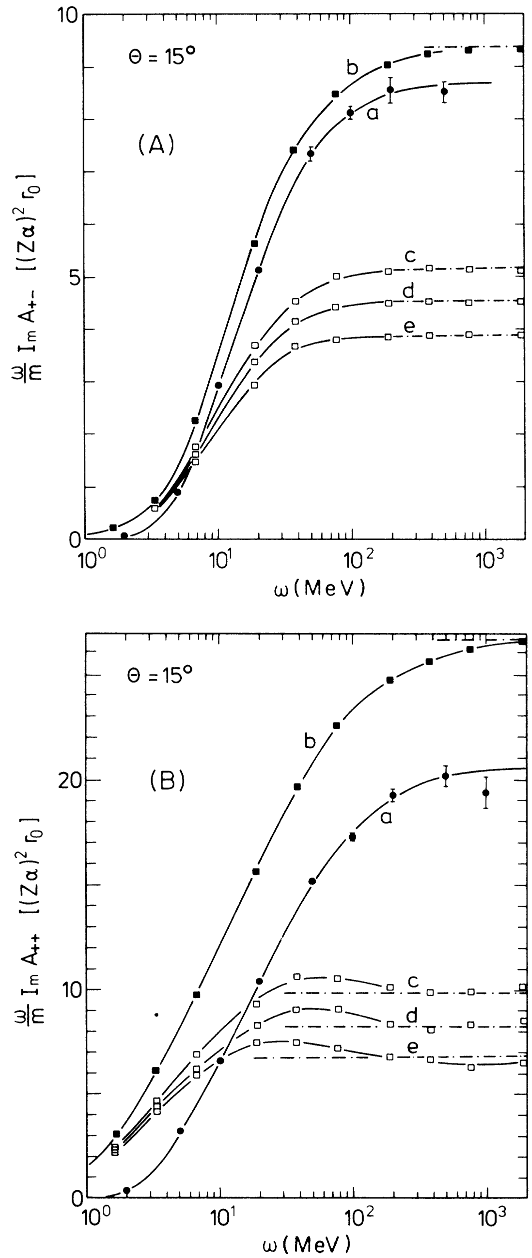

FIG. 4. Same as in Fig. 1 but for $\theta = 15°$.

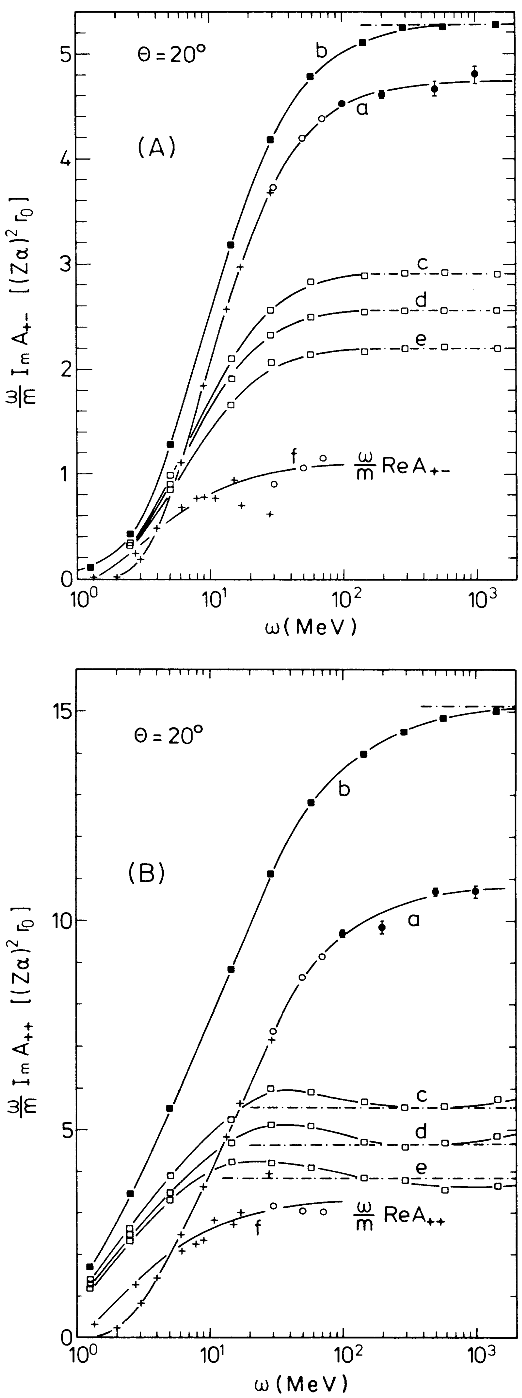

FIG. 5. Same as in Fig. 1 but for $\theta = 20°$.

the Coulomb-correction effect. As will be discussed in more detail in the next section these amplitudes showed an unexpected oscillatory behavior in the limit of high energies ω. In order to make sure that these oscillations were not artifacts of the Monte Carlo procedure, different variable transformations have been applied. The oscillations were present independent of the special form of the variable transformation as long as the Monte Carlo procedure lead to convergence.

IV. RESULTS AND DISCUSSION

The results of the present numerical investigation are summarized in Figs. 1–9. In Figs. 1–7 the data shown as squares and solid circles have been calculated by the present authors using the impact-factor method of Cheng and Wu[16,17] and the exact evaluation of the lowest-order Feynman graphs as given by De Tollis *et al.*,[11–14] respectively. Error bars attached to solid circles indicate the numerical accuracy achieved with the Monte Carlo procedure. The data denoted by crosses have been taken from the tabulation of Kahane *et al.*[15] Open circles are results of recent numerical calculations carried out by De Tollis *et al.*[14] The horizontal dash-dotted curves are from (8) and represent the impact-factor method in the

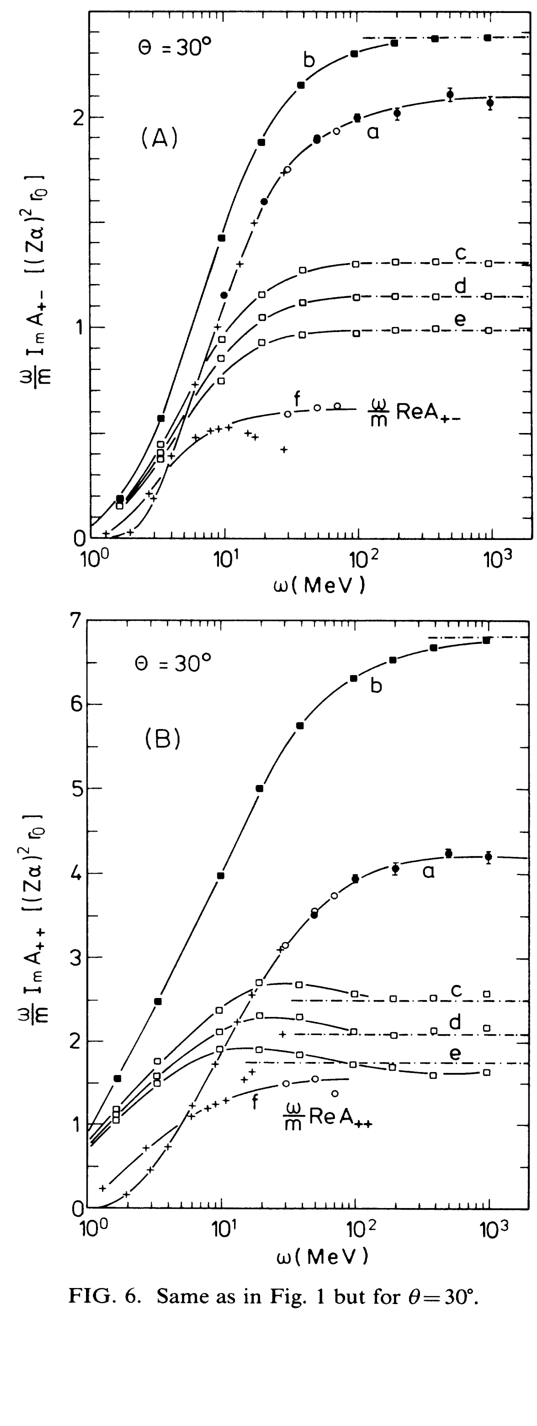

FIG. 6. Same as in Fig. 1 but for $\theta=30°$.

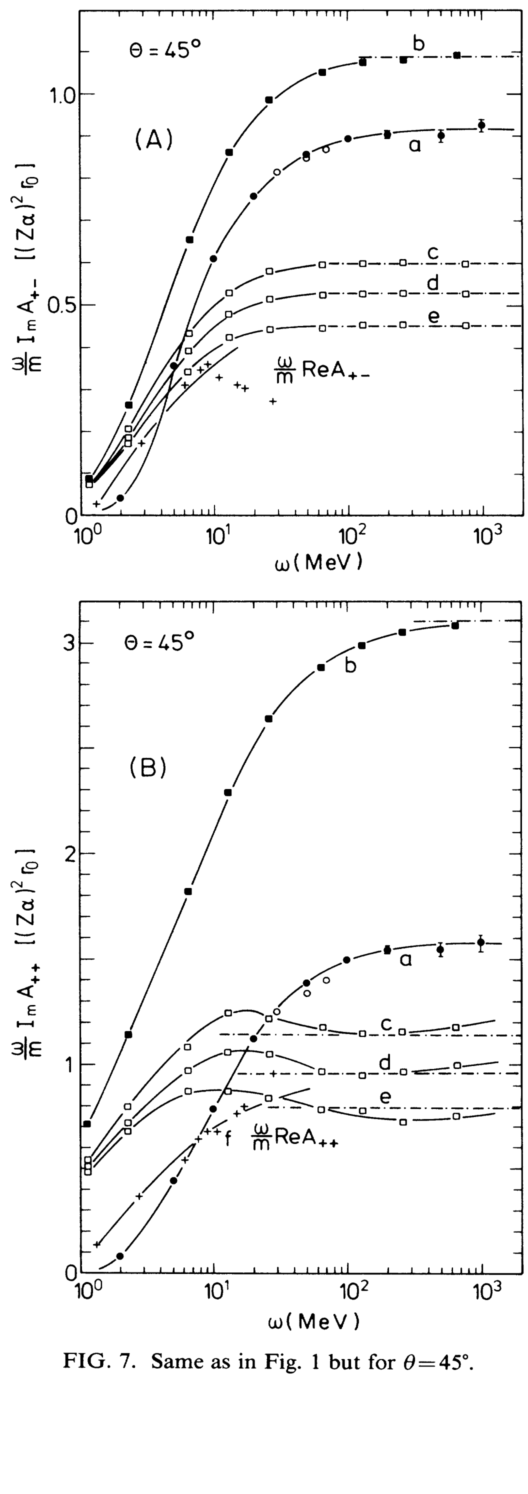

FIG. 7. Same as in Fig. 1 but for $\theta=45°$.

limit $\omega \gg \Delta \gg m$. The data of Fig. 8 are taken from the tabulation of Kahane *et al.*,[15] except for the data at 30, 50, and 70 MeV which were calculated by De Tollis and co-workers.[14] Solid curves are guides for the eye connecting or interpolating between data points.

For the lowest-order amplitudes we find a good agreement between the exact evaluation of the Feynman graphs (curves *a*) and the impact-factor method (curves *b*) for the very small scattering angle of $\theta=0.5°$. This agreement extends from the lowest energies of a few MeV to 10^4 MeV. With increasing scattering angle θ the amplitudes obtained from the impact-factor method become increasingly too large, the deviation from the exact lowest-order result being larger for the non-helicity-flip amplitude A_{++} than for the helicity-flip amplitude A_{+-}. Since $A_{++}=\frac{1}{2}(A_{\parallel}+A_{\perp})$ and $A_{+-}=\frac{1}{2}(A_{\parallel}-A_{\perp})$, it has to be one of the first two terms in the square brackets of Eq. (3.8) given in Ref. 17, i.e., the function $f(x,\sigma,z,z';\Delta)$ in (4) which contributes the largest part to this discrepancy.

Our findings concerning the properties of Delbrück amplitudes may be compared with the premises under which the different approaches have been obtained. The impact-factor method of Cheng and Wu[17] has been stated to be valid for

$$m \ll \omega \tag{9}$$

and

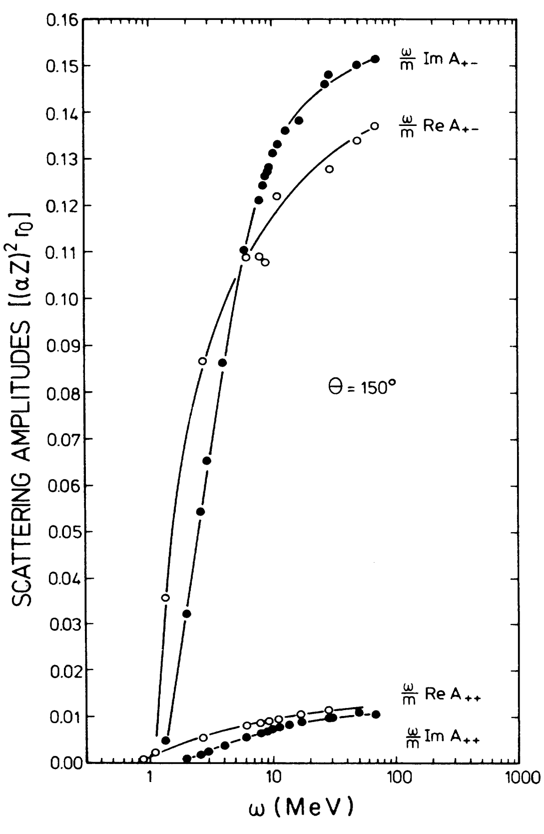

FIG. 8. Real and imaginary amplitudes for Delbrück scattering through $\theta=150°$ multiplied by ω/m, calculated from the exact evaluation of the lowest-order Feynman graph.

$$\frac{m^2}{\omega} \ll \Delta \ll \omega \tag{10}$$

and breaks down in the limit $\Delta \to 0$, a case which has been treated separately.[23] The scaling behavior has been stated to hold in the limits given by (9) and by

$$m \ll \Delta\ . \tag{11}$$

Equation (9) does not imply a serious restriction, since we are considering photon energies above a few MeV. In agreement with this expectation we do not find any discrepancy between the lowest-order predictions of Cheng and Wu[17] and De Tollis[11–14] in Fig. 1(a) and only a small energy-independent difference in Fig. 1(b). The statement $m^2/\omega \ll \Delta$ of (10) implies that the photon energy should be large in comparison with 6 MeV at $\theta=0.5°$, and large in comparison with 1 MeV at $\theta \geq 10°$. There is no indication in Figs. 1–7 that this restriction plays a role in the validity of the lowest-order predictions of Cheng and Wu.[17]

The only serious restriction of the validity of the impact-factor method stems from the inequality $\Delta \ll \omega$ in (10). Literally this inequality means that the scattering angle should be small compared to 60°. However, already at $\theta=5°$ there is a large discrepancy between the lowest-order predictions of De Tollis[11–14] and Cheng and Wu[17] in case of A_{++} [Fig. 2(b)], showing that the impact-factor method is accurate only at angles of one degree or less.

All the data shown in Figs. 1–7 clearly show indications of the scaling behavior predicted by Cheng, Tsai,

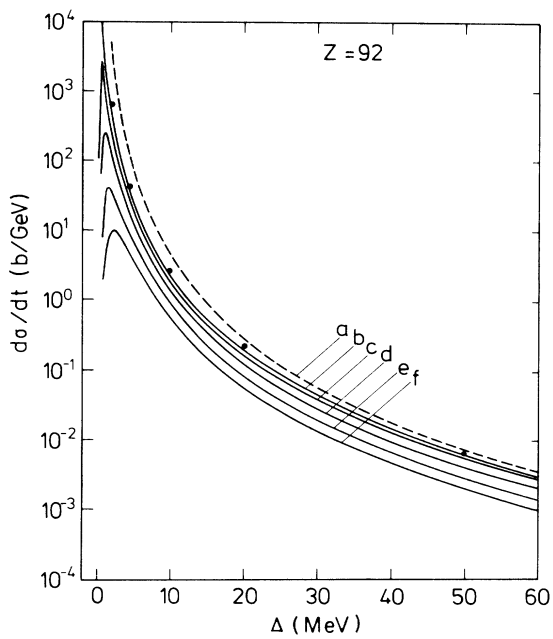

FIG. 9. Differential cross section for photon scattering calculated to lowest order. *a* asymptotic approximation (8) of the impact-factor method. Solid circles: Impact-factor method (4). *b–f* exact evaluation of the lowest-order Feynman graph for scattering angles of $\theta=0.5$, 5, 15, 30, and 45°, respectively. The ordinate is valid for $Z=92$.

and Zhu.[18] Furthermore, for the lowest-order as well as the Coulomb-corrected data obtained by the impact-factor method the asymptotic formula (8) depicted by dash-dotted lines seems to correctly represent the high-energy limit. In case of the non-helicity-flip amplitudes A_{++} the Coulomb-corrected data perform oscillations around the high-energy limits with amplitudes of the order of 10% or less. We do not believe that these oscillations are due to the Monte Carlo evaluation of the impact-factor method, because different weightings of the integration intervals lead to the same numerical results (see Sec. III).

Equation (11) may be used to predict lower limits for the photon energy above which the scaling behavior should show up. These lower limits are 60, 6, and 3 MeV for the scattering angles 0.5°, 5°, and 10°, respectively. For larger angles this lower-energy limit is 1 MeV or less. In Figs. 1–8 the scaling behavior shows up at much higher energies of the order of several hundred MeV for the lowest-order amplitude and between 10 and 100 MeV for the Coulomb-corrected amplitudes. The tendency of the data shown in Figs. 1–8 is that the lower-energy limit for the validity of the scaling behavior is shifted down with increasing scattering angle. At $\theta = 150°$ (Fig. 8) even the lowest-order amplitudes start scaling already well below 100 MeV. This tendency is in agreement with our former empirical findings.[19]

The impact-factor method provided us with information only for the imaginary amplitude. Indeed, at scattering angles $\theta \leq 20°$ the real amplitudes shown in Figs. 1–5 are always much smaller than the imaginary amplitudes. At larger angles the relative size of real parts increases and becomes equal to that of the imaginary parts at $\theta = 150°$ (Fig. 8).

Figure 9 shows differential cross sections $d\sigma/dt = (\pi/\omega^2)(d\sigma/d\Omega)$ for Delbrück scattering calculated in lowest order. The impact-factor method[16,17] predicts that $d\sigma/dt = (\pi/\omega^2)(d\sigma/d\Omega)$ depends on the momentum transfer Δ as the only parameter. The purpose of Fig. 9 is to explore to what extend this prediction is retained in the exact evaluation of the lowest-order Feynman graph.[9–14] By comparing curve b with the full circles, we see that at $\theta = 0.5°$ the exact evaluation of the Feynman graph approaches the predictions of the impact-factor method. This was known already from Fig. 1. However, the cross sections for larger angles, as depicted by curves c–f, show increasing deviations from curve b, especially for small momentum transfer. Therefore, $d\sigma/dt$ is found to depend on ω and θ separately, a property which may be of importance in the analysis of experimental data.

ACKNOWLEDGMENT

The calculations were performed at the Konrad Zuse-Zentrum für Informationstechnik, Berlin, on a Cray-1M. This work was supported by Deutsche Forschungsgemeinschaft (SFB 201 and Contract Schu 222).

---

*Present address: Fraunhofer Institut für Mikrostrukturtechnik, Berlin.

[1] P. Rullhusen, U. Zurmühl, F. Smend, M. Schumacher, H. G. Börner, and S. A. Kerr, Phys. Rev. C **27**, 559 (1983).

[2] R. Leicht, M. Hammen, K. P. Schelhaas, and B. Ziegler, Nucl. Phys. **A362**, 111 (1981).

[3] P. Rullhusen, W. Mückenheim, F. Smend, M. Schumacher, G. P. A. Berg, K. Mork, and L. Kissel, Phys. Rev. C **23**, 1375 (1981).

[4] G. Jarlskog, L. Jönsson, S. Prünster, H. D. Schulz, H. J. Willutzki, and G. G. Winter, Phys. Rev. D **8**, 3813 (1973).

[5] B. Kasten, D. Schaupp, P. Rullhusen, F. Smend, and M. Schumacher, Phys. Rev. C **33**, 1606 (1986).

[6] J. Kraus, Nucl. Phys. **B89**, 133 (1975).

[7] K. Ringhofer and H. Salecker, Found. Phys. **10**, 185 (1980).

[8] H.-D. Steinhöfer, Z. Phys. C **18**, 139 (1983).

[9] P. Papatzacos and K. Mork, Phys. Rev. D **12**, 206 (1975).

[10] P. Papatzacos and K. Mork, Phys. Rep. **21**, 81 (1975).

[11] V. Costantini, B. De Tollis, and G. Pistoni, Nuovo Cimento **2A**, 733 (1971).

[12] B. De Tollis, M. Lusignoli, and G. Pistoni, Nuovo Cimento **32A**, 227 (1976).

[13] B. De Tollis and G. Pistoni, Nuovo Cimento **42A**, 499 (1977).

[14] B. De Tollis and L. Luminari, Nuovo Cimento **81A**, 633 (1984).

[15] T. Bar-Noy and S. Kahane, Nucl. Phys. **A288**, 132 (1977).

[16] H. Cheng and T. T. Wu, Phys. Rev. Lett. **22**, 666 (1969)

[17] H. Cheng and T. T. Wu, Phys. Rev. D **5**, 3077 (1972).

[18] H. Cheng, E. C. Tsai, and X. Zhu, Phys. Rev. D **26**, 908 (1982).

[19] P. Rullhusen, U. Zurmühl, F. Smend, M. Schumacher, H. G. Börner, and S. A. Kerr, Phys. Rev. D **27**, 1962 (1983).

[20] M. Schumacher, F. Smend, P. Rullhusen, W. Mückenheim, and H. G. Börner, Instit. Phys. Conf. Ser. **62**, 598 (1981).

[21] M. Schumacher, in *Capture Gamma-Ray Spectroscopy and Related Topics—1984,* proceedings of the International Symposium, Knoxville, Tennessee, edited by S. Raman (AIP Conf. Proc. No. 125) (AIP, New York, 1985), p. 166.

[22] M. Ericson and M. Rosa-Clot, Z. Phys. A **324**, 373 (1986).

[23] H. Cheng and T. T. Wu, Phys. Rev. D **2**, 2444 (1970).